The University of Chicago

Limited Dispersal Drives Clustering and Reduces Coexistence by the Storage Effect

Jacob Usinowicz*

Department of Zoology, University of Wisconsin, Madison, Wisconsin 53706

ABSTRACT: Temporal variation can facilitate the coexistence of competitors through the temporal storage effect. However, this theoretical result was derived with the assumption that species have high dispersal rates. Here, I show that limited dispersal diminishes the storage effect in the classical lottery model. Populations become highly clustered during invasion, and population growth rates and extinction probabilities are functions of cluster size. I adopt the term "nucleation" from the physics literature to describe these characteristics. I developed approximations that incorporated nucleation to capture the spatiotemporal dynamics of the simulated model. Using analytical results from these approximations, I show that limited dispersal dampens asynchronous fluctuations in reproduction between species. This makes species appear to be more similar in their growth rate responses to the environment, thus reducing the potential for the storage effect. Theoretical results lead to simple rules relating average dispersal distances to relative reductions in potential coexistence. To demonstrate their use, I perform a preliminary analysis of two plant communities: tropical trees and desert annuals. In both communities, small-seeded species that disperse short distances on average have the strongest reductions in potential coexistence; species with wind- or animal-driven dispersal disperse farther distances, on average, and experience moderate or small reductions.

Keywords: dispersal, spatial pattern, coexistence, community dynamics, biological invasion, nucleation.

Introduction

Competition between species for shared resources can limit ecological diversity. The stable coexistence of multiple competitors requires competitive interactions to be stronger between conspecifics than between heterospecifics. This causes species to limit their own growth rates more strongly, preventing superior competitors from attaining the densities necessary to drive other species extinct (MacArthur and Levins 1967). Various mechanisms can promote coexistence in this way, including resource partitioning (MacArthur and

* E-mail: usinowicz@wisc.edu.

Levins 1964), frequency-dependent predation (Vance 1978), and the storage effect (Chesson and Warner 1981). However, the potential for coexistence can be affected if the dispersal of individuals or propagules is limited. These effects have been well enumerated for certain coexistence mechanisms, such as classic resource partitioning (Neuhauser and Pacala 1999; Bolker et al. 2003) and the spatial storage effect (Lavorel and Chesson 1995; Snyder and Chesson 2003), but are not as well understood in the context of other coexistence mechanisms, such as the temporal storage effect.

The temporal storage effect operates when fluctuations in species-specific growth rates and a long-lived stage work in concert to reduce interspecific, relative to intraspecific, competition (Chesson and Warner 1981). If growth rate fluctuations are sufficiently asynchronous, then each species will experience separate periods of favorable growth. This promotes intraspecific competition and decreases interspecific competition, because individuals compete primarily with conspecifics during these periods. However, interspecific competition only decreases relative to intraspecific competition if a long-lived stage is present to act as a buffer against the negative population growth that would otherwise occur during an unfavorable period (Chesson 2000b; Adler et al. 2006).

In many systems where the storage effect is important, individuals reproduce via propagules with limited dispersal ranges, as in grasses (Adler et al. 2006), desert annuals (Pake and Venable 1995; Angert et al. 2009), tropical trees (Kelly and Bowler 2002; Usinowicz et al. 2012), and potentially even coral reef fish (Chesson and Warner 1981). Limiting the movement of populations leads to spatial heterogeneity in the form of clusters of individuals (endogenous heterogeneity; Seidler and Plotkin 2006; Bolker 2003; Levine and Murrell 2003). The implications of this type of heterogeneity for coexistence by classic resource partitioning depend on certain characteristics of species. Coexistence may be facilitated when a superior competitor is more limited by dispersal (Bolker et al. 2003), but coexistence may be reduced when dispersal is symmetrical between species

(Neuhauser and Pacala 1999). These conclusions also depend on characteristics of the environment. If population growth rates of competitors are correlated with patchy resources (exogenous heterogeneity), dispersal limitation will increase the potential for coexistence (Snyder and Chesson 2003).

I constructed an explicitly spatial simulation model to investigate the impact of dispersal limitation on coexistence by the temporal storage effect. The simplest nonspatial model capable of producing the storage effect is the lottery model. Therefore, I adapted the lottery model for a discrete-space lattice, where each lattice square represents a colonization site capable of supporting a single reproductive individual. Offspring have a simple dispersal kernel, so that the offspring vying for an available site come only from a local interaction neighborhood, defined as the set of sites within dispersal distance. I analyzed the dynamics of the simulation model to understand how limited dispersal impacts the ability of one species to invade its competitor from low density, which is the signature effect of stabilizing coexistence mechanisms. I quantified spatial pattern on the basis of the density, size, and number of clusters for different parameter ranges. I then used a set of approximation techniques to identify specific ways in which spatial pattern mediates invasion rates.

Coexistence can be demonstrated using the invasion growth rate. This gives the expected population growth rate for a species recovering from low density (termed the invader) against established competitors (termed the residents). Coexistence is only possible if the invasion growth rate is positive for each species in turn (Turelli 1978; Chesson and Warner 1981). The overall bounds on coexistence can then be found by analyzing changes in the invasion growth rate across different parameter ranges. For some models, it is possible to find a mathematical expression for the invasion growth rate, often referred to as the invasion criterion. When the focus is on a specific scenario or system, this is not strictly necessary, because the invasion growth rate can be measured directly from field-parameterized simulations or models (Cáceres 1997; Adler et al. 2006; Angert et al. 2009; Godoy and Levine 2014). However, the invasion criterion can reveal which demographic features most strongly influence coexistence, potentially reducing complexity and focusing investigation on key parameters.

Deriving the invasion criterion for the limited-dispersal lottery model requires an analytically tractable version of the model. Thus I first approximate the spatial dynamics of the full model and then find the invasion criterion of the approximation. I compared a total of five approximations, including limited-dispersal and pairwise approximations with well-established histories of use in ecology (Hiebeler 1997, 2000; Ives et al. 1998), and three related approximations originating from the physics literature in

an area of research referred to as nucleation (Avrami 1940; White 1969; Korniss and Caraco 2005). Each approximation accounts for the influence of spatial pattern through an underlying model of the average interaction neighborhood. An approximation is successful when it matches the observed invasion growth rate of the limited-dispersal lottery model. The success of an approximation to represent dynamics during low-density growth can be seen as a test of the underlying model of spatial interactions. The invasion criterion for a successful approximation can then be used to infer which characteristics of competing species impact coexistence.

Nucleation theory provides a framework that can account for clusters and demographic stochasticity during growth from low density (Gandhi et al. 1999; O'Malley et al. 2005), both of which contribute to dynamics in the limited-dispersal lottery model. The three nucleation approximations adapted here share the assumption that population growth is cluster-based and recast dynamics as a series of transitions between cluster sizes. Each is applicable under different conditions: a transition matrix for a Markov chain that represents all possible transitions between cluster sizes and is most practical when spatial extent is small (White 1969); an exponential approximation, known as Avrami's law, that is accurate in the limit of very large lattices (Avrami 1940; Korniss and Caraco 2005); and a difference approximation, conceptually based on birth-death models (Gurney and Nisbet 1975; Snyder and Nisbet 2000), that considers the most likely cluster transitions for a given population size.

Demographic stochasticity is an important process to consider for the overall persistence of finite populations, because it can cause extinction even when species should otherwise be able to persist. However, the main goal here is to determine the impact of limited dispersal on the storage effect, which means distinguishing the contrasting impacts of demographic stochasticity from stabilizing coexistence. Nucleation theory provides a framework for simulating and analyzing low-density growth under these conditions by allowing a constant, low level of invader propagules to arrive wherever a resident dies (Korniss et al. 2000; Korniss and Caraco 2005). Many colonization attempts will fail, but eventually the invader will create a cluster of sufficiently large size to establish. This critical cluster size, c_c, divides these two phases of low-density growth. Below c_c growth is a random process with properties determined by the background propagule rate, lattice size, and species mortality rates. Above c_c, the invader population overcomes demographic stochasticity, and the growth rate is determined by competitive differences between species (Korniss and Caraco 2005); the growth rate above c_c is most comparable to the classic invasion growth rate.

The complexity of spatially explicit population models can make it difficult to connect results to empirical studies of real communities. Here, I adhere to the theoretical

framework of coexistence based on mutual invasibility (Turelli 1981; Chesson 2000b), since its applicability for analyzing empirical systems has been demonstrated. The most successful spatial approximation can be parameterized with field data in ways that are then directly comparable with previous studies (e.g., Adler et al. 2006; Angert et al. 2009; Usinowicz et al. 2012). Comparing the invasion criteria of the spatial approximations to that of the classic lottery model leads to simple rules for determining when dispersal limitation reduces the strength of the storage effect. Finally, I apply these results to a preliminary analysis of the impact of dispersal limitation on coexistence in two communities where the storage effect is important: desert annuals and tropical trees.

Although this article contains a substantial amount of technical development, the main results can be interpreted with the background provided in the introduction. Several quantities used to analyze cluster dynamics are introduced in the second part of "Methods," but their meanings are reiterated briefly in the corresponding "Results" sections. A more detailed summary of the framework of mutual invasibility is provided in the first "Methods" subsection, after the limited-dispersal lottery model is defined. The candidate spatial approximations are described in the final part of "Methods" whereas their derivations and the invasion criterion of each are found in the Appendixes (apps. A–C available online).

Methods

Limited-Dispersal Lottery Model

The limited-dispersal lottery model assumes that two species compete for fixed locations in space that can only be occupied by a single adult individual. Seed production by individuals of each species is variable through time. Here, I treat it as a random process where species have specific means and variances, and asynchrony between species is measured by an interspecific correlation coefficient. Seeds can only spread within a limited radius, and establishment (i.e., capturing a site to become an adult) can only occur at an empty site. Each generation, an individual seed chosen to establish at an empty site is picked at random from among all of the seeds at an open site; thus, a species' likelihood of capturing a site is proportional to the number of seeds present at that site. Because dispersal is limited, competition becomes locally limited to subsets of the population.

I modeled two species, a resident (species 0) and an invader (species 1), interacting on a square lattice of size L^2 with periodic boundary conditions; thus, a seed dispersing off the edge of the lattice is returned to the opposite side of the lattice. Each site on the lattice supports only a single individual of one species; at each time step t, a site z_{xy} takes

on a value of 0 or 1. Individuals die at a rate δ that is the same for both species. When an individual dies, its site is captured by either species probabilistically according to the relative numbers of seeds that individuals of each species disperse to that site. Capture occurs in the same time step at which mortality takes place, so there are no empty sites.

Reproductive adults of each species produce seeds at rates $R_0(t)$ and $R_1(t)$ in time step t. These rates are modeled as lognormally distributed random variables to constrain values to be positive, with means $\overline{R_0}$ and $\overline{R_1}$, variances σ_0^2 and σ_1^2, and correlation ρ between species, so that, taken together, they define the random vector $\boldsymbol{R}$. High covariance in $\boldsymbol{R}$ simulates species with similar responses to environmental fluctuations; reducing covariance (done by decreasing ρ in the following investigations) makes species increasingly different in their responses to the environment and increases the potential for the storage effect.

Seeds are dispersed according to a species-specific dispersal kernel $K(x, y; \Phi)$ describing the likelihood that any seed will travel a given distance from the parent plant. I model dispersal using a Moore neighborhood with a specified Chebyshev distance, and I later extend development to include more realistic (e.g., exponential) kernels (app. C). All sites within a predefined neighborhood $N_z = \{(z_a, z_b) : |z_a - z_x| < r_\varphi, |z_b - z_y| < r_\varphi\}$ receive $R_0(t)$ or $R_1(t)$ propagules from a reproductive adult centered at z_{xy}. The Chebyshev distance, which I refer to henceforth as the radius of dispersal r_φ, determines the distance (in units of sites) that propagules can travel. The diameter of dispersal $d_\varphi = 2r_\varphi + 1$, and the total area of N_z is given by $\Phi = d_\varphi^2$. The simplest kernel is $r_\varphi = 1$, in which case the dispersal kernel is a three-by-three block, centered on a reproductive adult plus its eight nearest neighbors (including corners).

The dispersal neighborhood N_z defines the interaction neighborhood, those individuals that can colonize a site made available by mortality. When the individual at z_{xy} dies, colonization is only possible by individuals in N_z. If there are $\eta_{1,xy}(t)$ adults of the invader species in N_z, then the colonization rate for the invader species at an empty site is the probability

$$\gamma_{xy}(t) = \frac{\eta_{1,xy}(t)R_1(t)}{\eta_{1,xy}(t)R_1(t) + (\Phi - \eta_{1,xy}(t))R_0(t)}. \quad (1)$$

The form of equation (1) is based on the assumption that mortality rates are equal between species and removes terms for the local resident population, $\eta_{0,xy}(t)$, from the equation by using $\Phi = \eta_{0,xy}(t) + \eta_{1,xy}(t)$. Species 1 has been defined as the invader, and species 0 has been defined as the resident.

Applying a mean-field approximation to the limited-dispersal model recovers the classic lottery model (app. A). Specifically, the dynamics of the limited-dispersal model approach those of the classic lottery model as dispersal be-

comes global (i.e., as $d_\varphi \rightarrow L$ and L goes to infinity). In the classic lottery model, the quantity $\gamma_{\mathrm{mf}}(t)$ represents the colonization probability for species 1,

$$\gamma_{\mathrm{mf}}(t) = \frac{p_1(t)R_1(t)}{p_1(t)R_1(t) + (1 - p_1(t))R_0(t)}. \tag{2}$$

The quantity $p_1(t)$, which replaces $\eta_{1,xy}(t)$ from equation (1), tracks the global population of the invader and is related to the population of the resident by $p_0(t) + p_1(t) = 1$. The form of $\gamma_{xy}(t)$ is nearly identical to $\gamma_{\mathrm{mf}}(t)$, the only difference being that interactions occur locally for the former and globally for the latter.

Stable coexistence requires that both species have positive population growth rates when recovering from low density. For the classic lottery model, invasion growth rates can be approximated analytically by considering what happens as either population approach zero, which leads to the classic expression (Chesson and Warner 1981)

$$E\left[\log\left(1 + \delta\left(\frac{R_1(t)}{R_0(t)} - 1\right)\right)\right] > 0. \tag{3}$$

Here $E[\ ]$ denotes an expectation over time. Although equation (3) is written in terms of the invader, this condition must be true for both species 1 and species 0 in turn as invaders for stable coexistence to be possible.

Simulations of the limited-dispersal lottery model are used directly to test for coexistence and measure invasion growth rates. Here, the invader is ascribed a constant, low-level introduction rate of propagules β to accommodate demographic stochasticity. Analyses presented here use $\beta = 10^{-4}$, unless otherwise noted. Thus, even in the absence of any reproductive adults (e.g., $p_1(t) \rightarrow 0$), the invader species will have a very small probability of colonizing an available site. Additionally, the invasion growth rate is measured as $p_1(t)$ approaches c_c in the simulation, whereas it is calculated as $p_1(t)$ approaches zero in the classic invasion growth rate. The value of c_c can be identified from simulations as the value of $p_1(t)$ at which a population is equally likely to reach its equilibrium population as it is to go extinct, and an analytical expression for c_c is derived in appendix B. Whenever coexistence is measured, this procedure is performed for both species 1 and species 0.

Spatial Pattern in the Limited-Dispersal Lottery Model

I used two common statistical measures to classify spatial pattern in the limited-dispersal lottery model. Moran's I quantifies clustering of the invader at the global scale by calculating correlations between neighbors (Moran 1950). It returns values ranging from −1 to 1, which are interpreted

analogously to standard (Pearson) correlation coefficients: negative values indicate nonrandom dispersion, because sites tend to be different than their neighbors (a checkerboard pattern at I = −1), and positive values indicate nonrandom clumping, because sites tend to be like their neighbors (complete segregation at I = 1). I also calculated the (empirical) semivariogram at each time step (Cressie 1993), which measures the degree of correlation between sites as a function of their separation distance instead of only nearest neighbors. I report the range of the semivariogram, r_s, which represents the maximum distance at which sites appear correlated (Cressie 1993), to indicate cluster size. The value of r_s was calculated by first finding the maximum value of the semivariogram and then determining the distance at which the semivariogram reached 95% of this value.

I investigated changes in these results as δ is varied across the range (0, 1) and ρ is varied across the range (−1, 1). In the classic lottery model, interspecific, relative to intraspecific, competition is determined by $\boldsymbol{R}$ and δ and more strongly by the former (Chesson and Warner 1981). More attention is paid to changes relative to $\boldsymbol{R}$; because δ is symmetrical and constant, it will only weakly influence invasion growth rates. Differences in σ_1^2 and σ_0^2 also contribute to coexistence, but these values are unbounded; therefore, it is more convenient to vary ρ to reproduce the full range of competitive dynamics. I calculated Moran's I and the semivariogram range, r_s, for different combinations of ρ and δ at three points of population growth: the critical radius from nucleation theory, twice the critical radius, and as species approach stochastic equilibrium (10^4 generations after populations have reached the size of twice the critical radius).

Nucleating systems demonstrate two distinct regimes of growth based on whether the population consists of a single cluster or multiple clusters. Population growth occurs through a single cluster when both L and β are small. Increasing either (or both) parameters eventually allows for multiple clusters (Rikvold et al. 1994; Richards et al. 1995; Korniss et al. 2000; Korniss and Caraco 2005). These two growth regimes are compared on the basis of $\langle t_i \rangle$, the time until establishment of the first critical cluster (the nucleation time), and t_g, the duration of invasive growth, defined as the time from $\langle t_i \rangle$ to predefined population threshold F. The value of F is set to half of the equilibrium density of the invader by convention (Richards et al. 1995; Korniss and Caraco 2005). An equation for the equilibrium density of the invader is given in appendix B.

Single-cluster growth is a Poisson process, and the time it takes to reach a specified population size during growth from low density is described by an exponential distribution. The cumulative distribution for $P_{\mathrm{inv}}(t)$, the probability of seeing an invader cluster of a given size, is as follows (Richards et al. 1995; Korniss and Caraco 2005):

$$P_{\text{inv}}(t) = \begin{cases} 0 & \text{for } t < t_{\text{g}} \\ 1 - \exp\left[-\dfrac{t - t_{\text{g}}}{\langle t_i \rangle}\right] & \text{for } t > t_{\text{g}} \end{cases}. \quad (4)$$

In the multicluster regime, the global density of the invader is a sum over many clusters, resulting in spatial averaging. This means that $P_{\text{inv}}(t)$ is Gaussian, and the corresponding cumulative distribution is given by the error function, $\text{erf} = 2\pi^{-1}\int_0^x e^{-t^2}\,dt$, with mean $\langle t_i \rangle$ and variance $\langle t_i^2 \rangle$ (Richards et al. 1995; Korniss and Caraco 2005):

$$P_{\text{inv}}(t) = 1 - \frac{1}{2}\left[1 + \text{erf}\left(\frac{t - \langle t_i \rangle}{\sqrt{2\langle t_i^2 \rangle}}\right)\right]. \quad (5)$$

I analyzed simulations of the limited-dispersal lottery model to determine whether the dynamics are consistent with these expectations across a range of parameter values. The presence of both regimes of cluster growth, fit by equations (4) and (5), suggests that nucleation dynamics are present in the model. I surveyed broadly across parameter space using a maximum-likelihood approach to fit parameters $\langle t_i \rangle$, t_{g}, and $\langle t_i^2 \rangle$, fixed $\beta = 10^{-4}$, and calculated the goodness-of-fit of equations (4) and (5) from $L = 16$ to 256 for each parameter combination; this should encompass both single- and multicluster regimes, if they exist. I recorded the value of R^2 to assess the goodness-of-fit and considered $R^2 > 0.98$ as a successful fit. Single- or multicluster growth was indicated by which equation provided a better fit at each L.

Spatial Approximations

I explored five approximations to the limited-dispersal lottery model, but only the nucleation approximations accurately represented the dynamics during low-density growth (see fig. A1; figs. A1, B1, B2 available online). For this reason, I leave the development of the local dispersal (LD) and pairwise approximations to appendix A. Here, I focus presentation on the nucleation difference approximation, formulated around the average rates of site addition and subtraction, which gives results that are comparable to the classic lottery model. The Markov chain and Avrami's law are conceptually related and give almost identical numerical results. However, they are not as comparable and are less likely to be applicable empirically. I include them for theoretical continuity with nucleation.

Nucleation describes population growth as a process in which clusters grow or shrink stochastically through addition and subtraction of sites. Dispersal distance, r_{φ}, defines the edge of a cluster. Population growth is constrained by interactions at the edge. Only a subset of resident-occupied sites at the outer edge of a cluster can be invaded; likewise, only a subset of invader-occupied sites at the inner edge of a cluster can be recolonized by the resident.

I define the subset of sites reachable by the invader as $N_{\text{I}}(p_1)$ and the subset reachable by the resident as $N_{\text{R}}(p_1)$; both are functions of invader population size. Each attempt to invade or recolonize occurs independently with probability $\gamma_{\text{I},xy}(t)$ and $\gamma_{\text{R},xy}(t)$, where subscripts distinguish sites in $N_{\text{I}}(p_1)$ being invaded and sites in $N_{\text{R}}(p_1)$ being recolonized. The net change in cluster size after all colonization attempts defines a transition from c_i to a new cluster: $c_i \to c_j$. The cluster transition probability λ_{ij} is a sum over all possible colonization attempts that can produce the transition $c_i \to c_j$. Each transition can be calculated from δ, $\gamma_{\text{I},xy}(t)$, and $\gamma_{\text{R},xy}(t)$. This rationale is expanded in appendix B with an example calculation.

It is more convenient to base approximations on average values of these quantities, given the increasing difficulty and time required to calculate λ_{ij} with larger clusters. For the limited-dispersal lottery model, this requires expressions for the average $\eta_{i,xy}$ of individuals in $N_{\text{I}}(c_i)$ and $N_{\text{R}}(c_i)$. This in turn requires expressions for the averages of $N_{\text{I}}(c_i)$, $N_{\text{R}}(c_i)$, and $N_{\text{M}}(c_i)$, which gives the number of invader-resident edges between $N_{\text{I}}(c_i)$ and $N_{\text{R}}(c_i)$. Then, $\overline{\eta_{\text{I}}(c_i)} = \overline{N_{\text{M}}(c_i)}/\overline{N_{\text{I}}(c_i)}$ and $\overline{\eta_{\text{R}}(c_i)} = \overline{N_{\text{M}}(c_i)}/\overline{N_{\text{R}}(c_i)}$, where overbar indicates the spatial average within the specified region. This allows $\gamma_{xy}(t)$ to be expressed as

$$\gamma_{\text{I}}(c_i) = E\left[\frac{\overline{\eta_{\text{I}}(c_i)}R_1(t)}{\overline{\eta_{\text{I}}(c_i)}R_1(t) + (\Phi - \overline{\eta_{\text{I}}(c_i)})R_0(t)}\right],$$

$$\gamma_{\text{R}}(c_i) = E\left[\frac{\overline{\eta_{\text{R}}(c_i)}R_{\text{R}}(t)}{\overline{\eta_{\text{R}}(c_i)}R_1(t) + (\Phi - \overline{\eta_{\text{R}}(c_i)})R_0(t)}\right]. \quad (6)$$

The subscripts I and R indicate $\gamma_{\text{I}}(c_i)$ and $\gamma_{\text{R}}(c_i)$ specific to $\overline{N_{\text{I}}(c_i)}$ and $\overline{N_{\text{R}}(c_i)}$, respectively. I develop expressions for the above quantities and support them with numerical results in appendix B.

The nucleation difference equation assumes that average transition rates, as a function of cluster size, are sufficient to capture invasion growth rates. Cluster growth is the sum of two processes: the number of sites gained and lost for c_i. On average, $\overline{N_{\text{I}}(c_i)}$ colonization attempts are made by the invader with average success probability $\delta\gamma_{\text{I},xy}$; this is a binomial process, with mean $\overline{B(p_1)}$. Likewise, the resident makes $\overline{N_{\text{I}}(c_i)}$ recolonization attempts on average each with probability of success $\delta\gamma_{\text{R},xy}$; this is also a binomial process, with mean $\overline{D(p_1)}$. Thus, the net invader growth rate is the difference between average births $\overline{B(p_1)}$ and deaths $\overline{D(p_1)}$,

$$p_i(t+1) = p_i(t) + \left[\overline{B(p_i)} - \overline{D(p_i)}\right]. \quad (7)$$

More detail and an expanded form of equation (7) are given in appendix B. It is worth noting that equation (7) and the definitions of $\overline{B(p_1)}$ and $\overline{D(p_1)}$ do not depend on the lottery model specifically.

The difference approximation can be solved to find c_c. The critical cluster is the population size at which the probabilities of growth and mortality are equal and can be found by setting $\overline{B(p_1)} - \overline{D(p_1)} = \delta$ and solving for $p_1 = c_c$. This produces a formula that is a function of dispersal distance (through the constants f, g, and h) as well as the reproduction rates $R_1(t)$ and $R_0(t)$. Due to its length, the formula for c_c is only given in appendix B.

A Markov chain approximation is developed by considering all possible transitions between cluster sizes explicitly and defining the transition matrix $\mathbf{P}$ (White 1969), instead of considering only average transition probabilities. Entries λ_{ij} of $\mathbf{P}$ give the probability of seeing a transition from cluster size j to cluster size i. The stationary distribution of $\mathbf{P}$ can be solved to obtain the matrix of mean first-passage times $\mathbf{M}$ (Kemeny and Snell 1960; Roberts 1976), where each entry M_{ij} gives the average time required for a cluster initiated at size c_i to grow to c_j. The useful quantities obtained from $\mathbf{M}$ include the nucleation rate $\langle t_i \rangle$ as M_{1c} and the duration of invasive growth t_g as M_{cF}. See appendix B for more details.

The matrix of transition times is most useful in conjunction with an approximation known as Avrami's law, which introduces the additional assumption that L is large enough for multiple clusters. It has been applied in the context of phase transitions of crystallizing solids (Rikvold et al. 1994), ferromagnetic materials (Ishibashi and Takagi 1971), and ecological invasion (Korniss and Caraco 2005) to predict changes in the global density of an invader. Avrami's law is stated as follows:

$$p_i(t+1) \approx 1 - \exp\left[-\ln(2)\left(\frac{t}{\langle \tau \rangle}\right)^3\right], \qquad (8)$$

where $\langle \tau \rangle = t_g + \langle t_i \rangle$ is referred to as the metastable lifetime. The value of $\langle \tau \rangle$ can be determined from $\mathbf{M}$ as M_{1F}. Alternatively, $\langle \tau \rangle$ can be measured directly from data on cluster growth by fitting equation (4).

Results

Spatial Pattern in the Simulation Model

Before investigating the impact of dispersal limitation on the storage effect, it is worthwhile to establish the properties of spatial pattern produced by the model. Population growth is driven by the initiation and expansion of clusters across broad parameter ranges. Figure 1 shows several realizations of the limited-dispersal lottery model for the specific case when $\delta = 0.9, \overline{R_1} = 1, \overline{R_0} = 1.01, \sigma_1 = \sigma_0 = 1,$
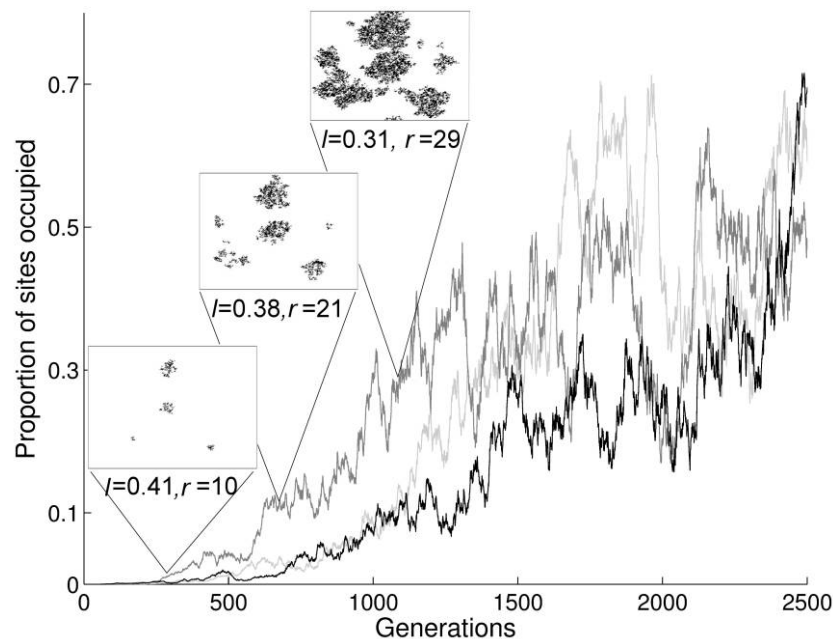

Figure 1: Three simulated invasions are shown for the limited-dispersal lottery model on a large lattice with a low background invasion rate ($L = 256, \beta = 10^{-4}$). The growth rates R_1 and R_0 are simulated as lognormal random variables with means $\overline{R_1} = 1$ and $\overline{R_0} = 1.01$, variances $\sigma_1^2 = \sigma_0^2 = 1$, and correlation $\rho = 0$. Dispersal is among neighboring cells only ($\Phi = 9$). The insets show the growth of clusters at three randomly chosen time points during invasion. Below each inset, Moran's I and the semivariogram range r_s are given as measures of spatial correlation with nearest-neighbors and the maximum correlation distance between sites, respectively.

$\rho = 0$, $\beta = 10^{-4}$, and $L = 256$. Clusters are evident when inspecting the lattice (insets) and are supported by Moran's I and the semivariogram range, r_s. Cluster properties of the invader are dynamic during recovery from low density. Moran's I decreases from a mean ($\pm$ SD) of 0.41 ± 0.09 to 0.32 ± 0.07 as invader clusters coalesce to span the lattice at population sizes $> L^2/2$. The value of r_s increases from a measured value of 10.1 ± 6.7 to a maximum of 225 ± 28.9 as clusters coalesce (fig. 1). Dynamic, cluster-driven growth was present at every examined parameter combination, and the properties of clusters vary only subtly when changing the intensity of interspecific interaction by varying ρ or δ (results not shown).

The match of the observed cluster dynamics to that predicted by nucleation theory provides evidence of nucleation dynamics. Both single and multicluster growth regimes are present when L and β are varied and other parameters are fixed (fig. 2). A single-cluster regime was identified by fitting equation (4) to the cumulative distribution of wait times for the resident population, $P_{inv}(t)$. The multicluster regime was identified using equation (5) to fit the cumulative distribution of $P_{inv}(t)$. The R^2 goodness-of-fit for both equations (4) and (5) was calculated for 1,000 simulations at each order of magnitude from $\beta = 10^{-2}$ to $\beta = 10^{-6}$, with all other parameters fixed at $\delta = 0.9$, $\overline{R_1} = 1$, $\overline{R_0} = 1.01$, $\sigma_1^2 = \sigma_0^2 = 1$, $\rho = 0$, and $L = 32$. Values above $\beta = 10^{-4}$ were fit better by equation (4) ($R^2 > 0.98$), indicating lattices in the single-cluster regime, whereas values below $\beta = 10^{-4}$ were within the multicluster regime ($R^2 > 0.98$). At $\beta = 10^{-4}$, both equations fit with equivalent R^2 values, reflecting the fact that the transition from single to multicluster regime is continuous. Near $\beta = 10^{-4}$, enough clusters are present to make equation (4) a less adequate fit, but there are not yet enough clusters to make equation (5) a good fit. This goodness-of-fit test produced equivalent results to the example reported here across a broad range of parameter values (results not shown). Thus, recovery from low density always appears to occur through nucleation in the limited-dispersal lottery model.

Changing species similarity in their environmental response by varying ρ also changes the shape of the cumulative distributions, equations (4) and (5). Figure 2A shows examples of the cumulative distribution of $P_{inv}(t)$ on a log-linear scale in the single-cluster regime ($L = 32$) for $\rho = -0.8$, 0, 0.8, and figure 2B shows example fits in the multicluster case ($L = 256$) for the same values of ρ. The change in curvature across ρ reflects an increase in interspecific relative to intraspecific competition and an accompanying decrease in invasion growth rates; when competition is more intense, invasive growth is slower, translating into a lower probability that an invader species has reached the predefined population threshold F in a certain number of generations.

Invasion Growth Rates

The growth rate of an invader is lower in simulations of the limited-dispersal lottery model, relative to the classic lottery model. This means that dispersal limitation tends to increase the strength of interspecific, relative to intraspecific, competition an invader experiences. Figure 3A demonstrates this result for the specific case when $\delta = 0.9$, $\overline{R_1} = 1$, $\overline{R_0} = 1.01$, $\sigma_0^2 = \sigma_1^2 = 1$, $\rho = 0$, $\beta = 10^{-4}$, and $L = 256$. Here, the mean invasion growth rate ($\pm$ SD) was $0.0092 \pm .0011$ for the limited-dispersal simulation model calculated from 3,000 runs. The invasion growth rate was 0.0676 for the lottery model. These invasion growth rates were best approximated by the nucleation approximations: Avrami's law slightly underpredicted at 0.0088, and the difference approximation slightly overpredicted at 0.0108.

The impact of dispersal limitation was greatest on invasion growth rates when species responses to environmental fluctuations, as measured by ρ, were the most different. Figure 3B shows that the difference between invasion growth rates of the limited-dispersal and classic lottery model increased with decreasing ρ. Decreasing ρ permits each species to have an increasing number of recruitment events where it is favored over its competitor, which in turn increases invasion growth rates and reduces interspecific relative to intraspecific competition. This increasing difference in invasion growth rate between models indicates that species advantages during favorable recruitment events are substantially diminished by limited dispersal.

Invasion Criteria

Deriving the invasion criterion for the nucleation difference approximation reveals the mechanism that reduces invasion growth rates in the limited-dispersal lottery model (eq. [B18]). This invasion criterion can be compared to that of the classic lottery (eq. [3]) in terms of a damping coefficient D_N multiplying $R_1(t)/R_0(t)$, the invader relative advantage in a generation, of equation (3):

$$D_N = \frac{(fc_c + h_I)(gc_c + h_M)}{c_c\{\Phi(fc_c + h_I) + (gc_c + h_M)[(R_1(t)/R_0(t)) - 1]\}}$$
$$- \frac{R_0(t)}{R_1(t)}\left(\frac{(gc_c + h_M)}{(gc_c + h_M)[1 - (R_1(t)/R_0(t))] + \Phi c_c(R_1(t)/R_0(t))} - 1\right).$$
$$(9)$$

The constants f and g relate cluster size to the average neighborhoods $\overline{\eta_I(p_i)}$ and $\overline{\eta_R(p_i)}$ experienced by sites in $N_I(p_i)$ and $N_R(p_i)$, respectively: $f \approx d_\varphi$ and $g \approx d_\varphi(d_\varphi - 1)$. The constants h_I and h_M contain additional terms that are important when the invader population is very small and are used to constrain the average neighborhoods so that $N_I(1) = 1$ and $N_R(1) = (\Phi - 1)$. See appendix B for more details. Damp-
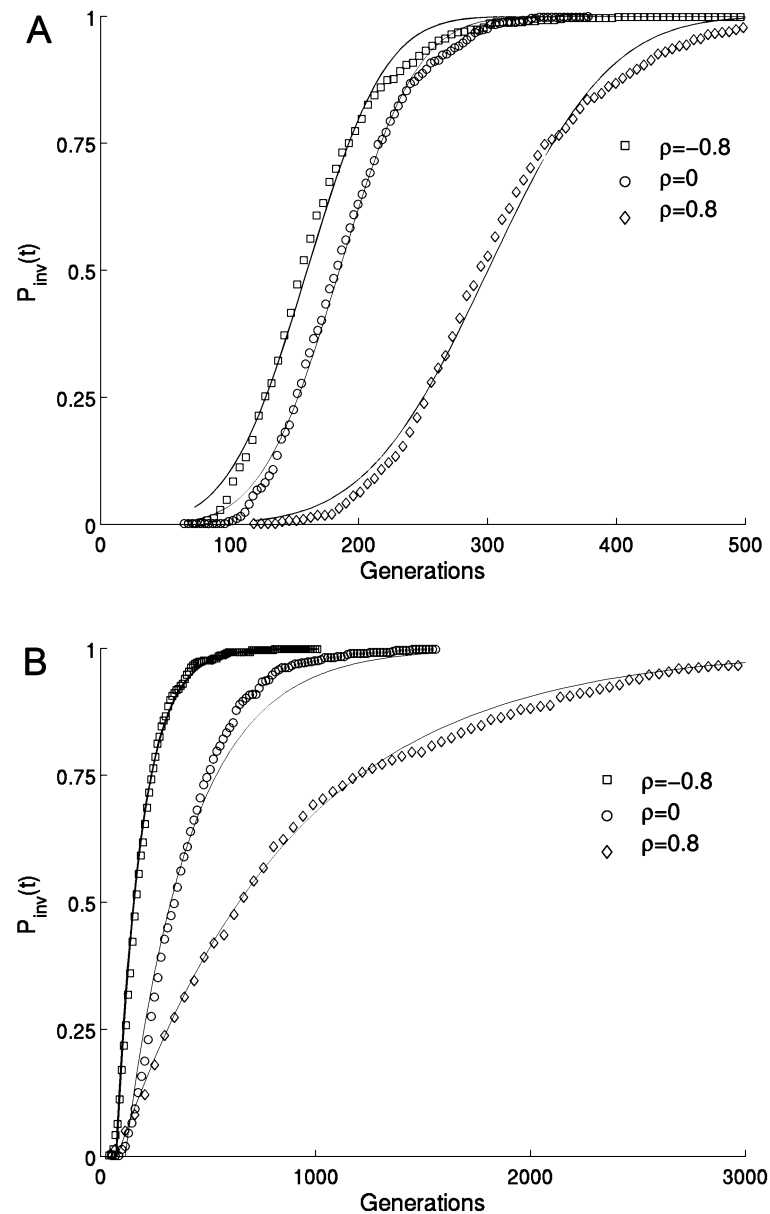
Figure 2: Cumulative probability $P_{\text{inv}}(t)$ that the invader species has reached a certain size ($0.1 \times$ equilibrium density) by a given time in the limited-dispersal lottery model. Panels show the cumulative distributions in either the single-cluster (*A*) or multicluster (*B*) regime. Results are based on 1,000 simulations with parameter values $\delta = 0.9, \overline{R_1} = 1$, and $\overline{R_0} = 1.01$, $\sigma_0^2 = \sigma_1^2 = 1$, $\rho = 0$ and $\beta = 10^{-4}$. When $L = 32$, the single-cluster distribution (*A*) is best fit as a Poisson (filled circles, with solid best-fit curve); when $L = 256$, the multicluster distribution (*B*) is best fit as a Gaussian distribution (open squares, with dashed best-fit curve). Examples of the cumulative distributions in *B* and *C* show that increasing ρ creates longer wait times, reflecting an increase in interspecific relative to intraspecific competition.

ing coefficients for the other approximations are given in appendix A.

The magnitude of D_N is a function of invader advantage in a recruitment event (fig. 4*A*). When the invader has the advantage ($R_1(t)/R_0(t) > 1$), then $D_N < 1$, and its advantage is reduced. When the resident has a high recruitment event

$(R_1(t)/R_0(t) < 1)$, then $D_N > 1$, and the reciprocal effect is observed for the resident. Coexistence in the classic lottery model is driven by $R_1(t)/R_0(t)$. Species 1 has positive growth when $R_1(t)/R_0(t) > 1$ and must have $R_1(t)/R_0(t) > 1$ on average to invade successfully; coexistence requires that species 0 also have $R_0(t)/R_1(t) > 1$ on average when it is invading
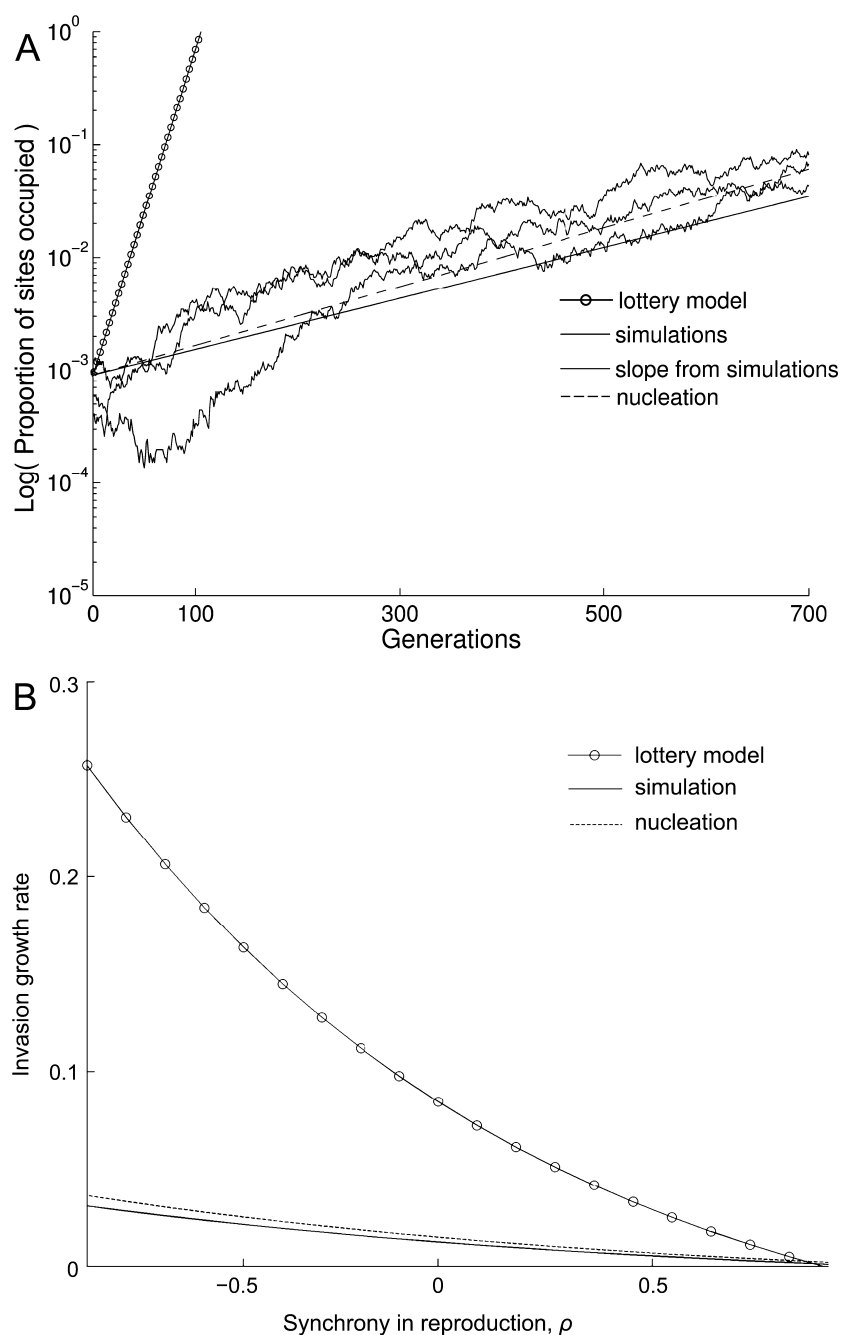
Figure 3: Invasion growth rates (*A*) and the relative change in invasion growth rates with increasing competition (*B*) for the simulated limited-dispersal lottery model, classic lottery model, and the nucleation difference approximation. *A*, Three example runs of the simulation are plotted against a mean ($\pm$ SD) log-linear slope fit from 3,000 runs (0.0092 ± 0.0011). The invasion growth rate predicted by the classic lottery model (mean-field approximation) is much larger (0.0676). The nucleation difference approximation provides the best match to the actual invasion (0.0108). *B*, Decreasing ρ simulates the case when species become more different in their response to environmental fluctuations. The impact of dispersal limitation increases as ρ decreases, evidenced by the difference between invasion growth rates in the classic lottery model and the limited-dispersal lottery model. This indicates that dispersal limitation decreases the strength of the storage effect because it reduces species advantages during favorable recruitment periods, making species appear more similar in their response to environmental fluctuations. Parameter values are as follows: $\delta = 0.9$, $\overline{R_1} = 1$, $\overline{R_0} = 1.01$, $\sigma_0^2 = \sigma_1^2 = 1$, $\rho = 0$, $L = 256$, and $\beta = 10^{-4}$.
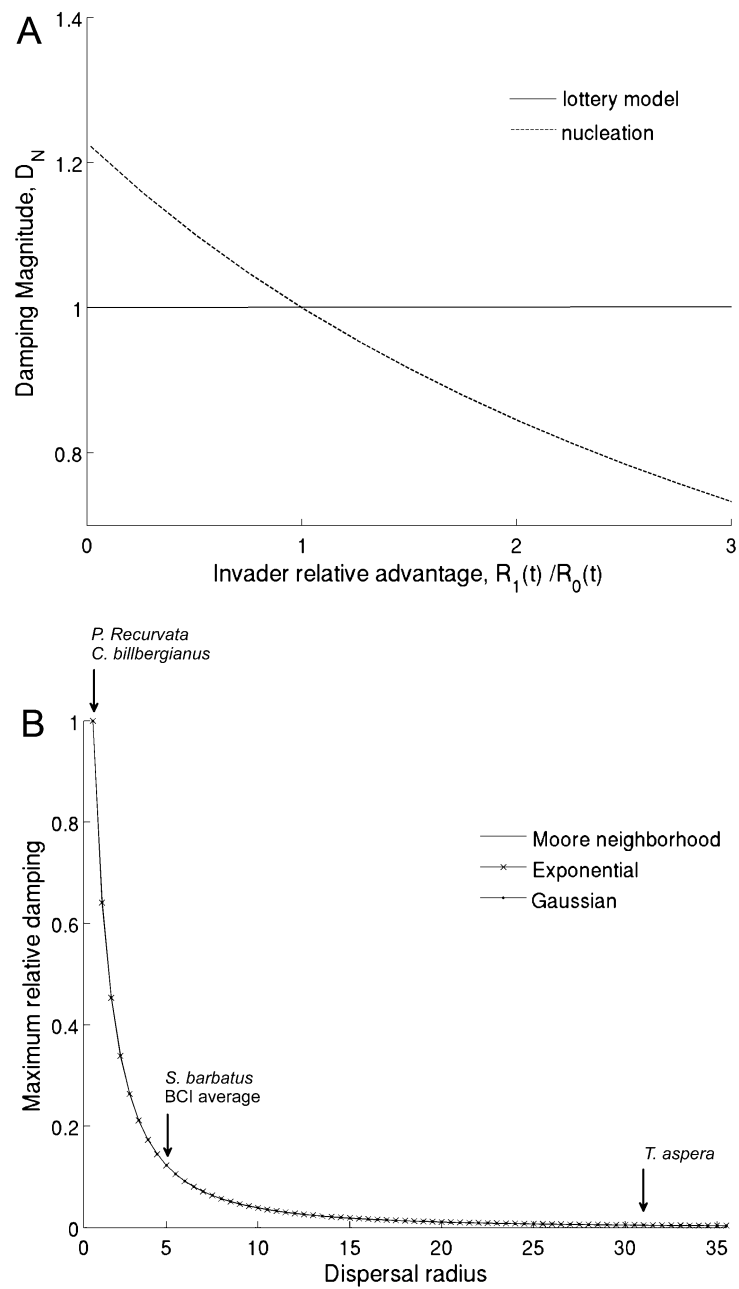
Figure 4: The impact of dispersal limitation as captured by the damping coefficient in the invasibility criterion of the nucleation difference approximation (*A*) with respect to dispersal distance (*B*). *A*, Relative magnitude of damping in the nucleation difference approximation D_N (dotted line) and the classic lottery model (horizontal line at 1) as function of per-generation invader relative advantage $R_1(t)/R_0(t)$. When the invader produces more potential recruits, D_N decreases its advantage but also reduces the resident advantage when it produces more potential recruits. *B*, Damping effect of D_N decreases as (average) dispersal distance increases. This is summarized using $D_{N,0}(d_\varphi)$, which gives the magnitude of D_N when $R_1(t)/R_0(t) = 0$; in this case, the resident will experience the strongest damping effect (the reciprocal case for the invader occurs when $R_0(t) = 0$ and the damping is $1/D_{N,0}(d_\varphi)$). The *Y*-axis is scaled relative to the strongest damping effect $D_{N,0}(3)$. This change is the same when dispersal is modeled with exponential and Gaussian dispersal kernels (for these kernels, r_φ corresponds to average dispersal distance). Arrows place results from the preliminary analysis: *Pectocarya recurvata* ($d_\varphi = 3$) and *Scleromystax barbatus* (11) are desert annuals (Venable et al. 2008), *Croton billbergianus* (3) and *Thelidomus aspera* (63) are tropical trees, and BCI average gives the overall average dispersal distance at Barro Colorado Island (11).

643

against species 1. Thus D_N will reduce the overall importance of these events and reduce the likelihood that these conditions for coexistence are met.

Analysis of D_N as d_φ increases provides insight into the conditions under which dispersal limitation has the most impact on coexistence. Expanding equation (9) shows that D_N is driven by lead terms in the numerator of $d_\varphi^5 c_c^3 + d_\varphi^4 c^2 \{h_I + c_c[(R_1(t)/R_0(t))-1]\}$, and similarly in the denominator $d_\varphi^5 c_c^3 + d_\varphi^4 c^2 \{h_I + 2c_c[(R_1(t)/R_0(t))-1]\}$. When d_φ is small, terms less than fifth order drive the damping effect. The fourth-order terms are nearly identical except for the factor of 2 in the denominator; this will cause the denominator to be noticeably larger (when $R_1(t) > R_0(t)$) or smaller (when $R_1(t) < R_0(t)$) relative to the numerator. As d_φ increases, the damping effect diminishes, because the identical fifth-order terms in the numerator and denominator overwhelm the lower-order terms, and $D_N \approx 1$.

The behavior of D_N as it approaches 1 provides insight into the impact of dispersal limitation on invasion growth rates and the storage effect. This can be summarized by considering the change in D_N when $R_1(t)/R_0(t) = 0$, abbreviated henceforth as $D_{N,0}(d_\varphi)$. At $D_{N,0}(d_\varphi)$, the resident will experience the strongest damping effect; given the symmetry assumptions of the model, the strongest damping effect on the invader should approach $1/D_{N,0}(d_\varphi)$. Because $D_{N,0}(d_\varphi)$

is an analytical limit of the magnitude of damping, it is indicative of the maximum amount by which dispersal limitation can reduce potential coexistence. Values of $D_{N,0}(d_\varphi)$ are plotted against a range of dispersal distances in figure 4*B*. The maximum value of $D_{N,0}(d_\varphi)$ is obtained at $d_\varphi = 3$ ($D_{N,0}(3) = 1.35$); at $d_\varphi = 7$, the effect of $D_{N,0}(d_\varphi)$ has already decreased 64% ($D_{N,0}(7) = 1.13$), and by $d_\varphi = 20$, it has decreased 90% ($D_{N,0}(20) = 1.04$).

Coexistence

The relative increase in interspecific, relative to intraspecific, competition created by dispersal limitation decreases the potential for coexistence by the storage effect in comparison to the classic lottery model. The strength or potential for coexistence can be quantified in relation to the fitness difference between species, quantified here as the ratio $\overline{R_1}/\overline{R_0}/\overline{R_0}$. The distance between the upper and lower coexistence bounds on $\overline{R_1}/\overline{R_0}$ provides a measure of the magnitude of the storage effect. Larger fitness differences are tolerated when the magnitude of the storage effect is higher; thus, I refer to the bounds on $\overline{R_1}/\overline{R_0}$ as measure of the strength of the storage effect (Chesson 2000*b*). Figure 5 shows the change in bounds on $\overline{R_1}/\overline{R_0}$ as ρ is increased to make species more similar in their reproductive response to the environment.
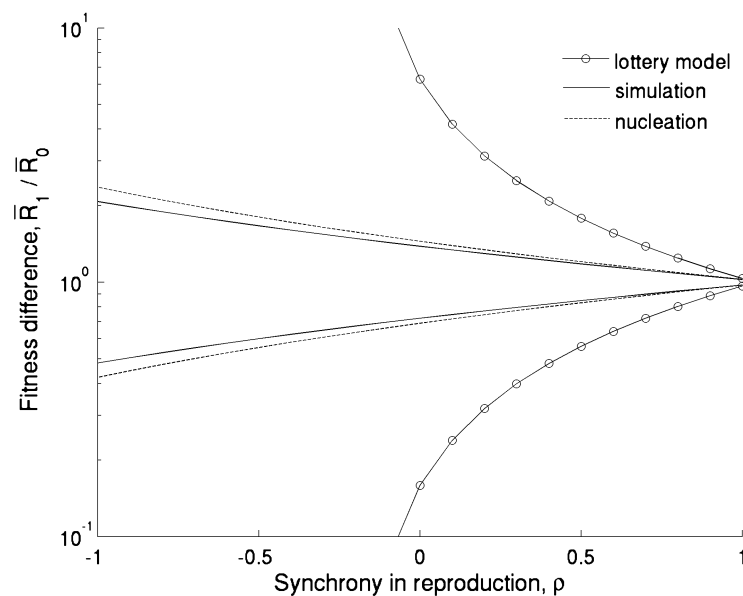

Figure 5: Coexistence bounds as a function of the fitness difference $\overline{R_1}/\overline{R_0}$ and interspecific correlation in reproduction rates ρ. Each pair of curves gives the upper and lower bounds on $\overline{R_1}/\overline{R_0}$ that permit coexistence. The distance between upper and lower bounds measures the total strength δ of the storage effect as a function of ρ and other key parameters of the model (δ, σ_0^2, σ_1^2). The curves converge on the line at $\overline{R_1}/\overline{R_0} = 1$; when growth rates are equivalent, coexistence is possible regardless of how similar species are. Coexistence is reduced in the limited-dispersal model, relative to the classic lottery model. The nucleation approximations provide the most accurate prediction of species coexistence (nucleation difference approximation shown). Parameter values are as follows: $\delta = 0.9$, $\overline{R_1} = 1$, $\overline{R_0} = 1.01$, $\sigma_0^2 = \sigma_1^2 = 1$, $\rho = 0$, $L = 256$, and $\beta = 10^{-4}$.

The distance between bounds increases as ρ approaches -1 for each model, showing the increased strength of the storage effect. However, the total area from $\rho = -1$ to $\rho = 1$ is larger for the classic lottery model than it is for the limited-dispersal model.

Preliminary Analysis of Dispersal-Limited Communities

I used the above results to perform a preliminary analysis of reduction in the potential for the storage effect in two dispersal-limited plant communities: desert annuals (Pake and Venable 1995; Chesson et al. 2004; Angert et al. 2009) and tropical forests (Usinowicz 2012). This analysis first requires adaptation of theoretical results to accommodate more biologically realistic dispersal kernels. Minor changes in $\eta_1(p_i)$ and $\eta_R(p_i)$ lead to slight differences in D_N (app. C). Results for exponential and Gaussian dispersal kernels (Clark 1998) are shown in figure 4B. The change in $D_{N,0}(d_\varphi)$ for these dispersal kernels was nearly identical to Moore neighborhoods, indicating that there is almost no difference in overall behavior of the system. The average dispersal distance of each exponential kernel was used for r_φ, calculated according to equation (4) of Clark et al. 1998. Dispersal kernels have been fit for certain desert annuals and tropical trees (Muller-Landau et al. 2008; Venable et al. 2008). From these studies, I obtained mean dispersal distances, which I scaled by adult size to adapt field measurements to units more similar to the theoretical model (i.e., in units of adult territory). These scaled average dispersal distances were used as species-specific values of r_φ ($d_\varphi = 2r_\varphi + 1$). Using $D_{N,0}(d_\varphi)$ (fig. 5A), it was then possible to approximate the potential impact of dispersal limitation.

The reduction in the storage effect from dispersal limitation is likely to be higher in desert annuals, although some tropical trees can be very dispersal limited. The desert annuals *Pectocarya recurvata* and *Schismus barbatus* (Venable et al. 2008) have dispersal radii r_φ of approximately 0.7 m/0.15 m ≈ 5 units and 0.29 m/0.2 m ≈ 1 unit, respectively. The dispersal kernels of 44 species from the tropical forest of Barro Colorado Panama (BCI) have been fit (Muller-Landau et al. 2008), which can be scaled relative to typical adult crown width (O'Brien et al. 1995) to give a community-wide average for r_φ of 5 (11) units (21 m/4 m), a minimum r_φ of 1 (3) unit (5 m/4 m) for *Croton billbergianus*, and a maximum r_φ of 31 (63) units (125 m/4 m) for *Trattinnickia aspera*. Interpreting from $D_{N,0}(d_\varphi)$ (fig. 5B), dispersal limitation will strongly reduce the storage effect when *S. barbatus* competes against similar species, whereas *P. recurvata* experiences only about 20% of this effect. At BCI, *C. billbergianus* will experience a strong reduction in the storage effect from dispersal limitation, but most species will experience <20% of this effect, and *T. aspera* experiences only 1.3% of this effect.

Discussion

Limited dispersal can reduce the potential for coexistence in the lottery model by preventing species from accessing sites for recruitment. This leads to a loss in reproductive effort; at the extreme that no open sites are within dispersal distance, a species experiences zero recruitment regardless of how much they reproduce. In theoretical analyses, this is captured through a damping coefficient that increasingly reduces the advantage of either species as recruitment periods become more favorable (fig. 4A). Averaged over many recruitment events, this decreases invasion growth rates (fig. 3A) and reduces the potential for coexistence (fig. 5). Species that differ markedly in their environmental response (i.e., that have low ρ) are the most strongly affected (fig. 3B). In biological terms, dispersal limitation makes species with different reproductive responses to the environment appear more similar in their recruitment rates, thus diminishing the potential for the (temporal) storage effect.

Nucleation theory was successful in characterizing the dynamics of the limited-dispersal lottery model. Not only were clusters present in simulations (fig. 1), but both single- and multicluster growth regimes were observed when spatial extent and background propagule rate were varied, and the progression of cluster growth was fit by models from nucleation theory (fig. 2). The nucleation approximations best captured the impact of dispersal limitation on invasion growth rates (fig. B1) and coexistence (fig. B2). By recasting population growth as a transition between cluster sizes, interactions at the scale of the local neighborhood are highly constrained to represent the edge of the growing cluster. In comparison, assuming that sites are independent (local dispersal) or that pairs of sites are independent (pairwise) lets species seem more evenly dispersed, and thus an invader will seem to have more access to sites. Because there is almost no difference among the nucleation approximations in their ability to represent spatial dynamics, these approximations can be used interchangeably according to the data available. However, the Markov chain approximation and Avrami's law are not as likely to be useful in an empirical setting because of the intensity of data needed for fitting, and thus they serve primarily to make the theoretical connection to nucleation more explicit.

Species that disperse propagules farther experience greater potential for coexistence by the temporal storage effect (fig. 4B). For the investigations here, the classic lottery model represents an upper limit on the strength of this mechanism, because global dispersal allows species to take full advantage of periods of high reproductive output. The farthest-dispersing species are the closest to this limit, as in the case of *Trattinnickia aspera*, a tropical tree included in the preliminary analysis with an average dispersal distance of 125 m. Many

other species are less able to capitalize on recruitment fluctuations but still only experience small reductions in the potential for the storage effect. Small-seeded species with mechanistic dispersal methods (i.e., not by wind or animals) typically disperse the shortest distances (Levin et al. 2003) and are therefore the least likely to depend on the temporal storage effect for coexistence. These results suggest that the storage effect may be more important in communities such as tropical forests, where species disperse long distances on average (Seidler and Plotkin 2006; Muller-Landau et al. 2008). This provides theoretical support for the importance of long-distance dispersal mechanisms in plant communities (Seidler and Plotkin 2006), especially instances where animals have been shown to disperse preferentially to gaps (Howe and Smallwood 1982); these forms of dispersal increase the likelihood that propagules will find available sites.

Dispersal limitation can have contrasting effects on coexistence, depending on features of species and their environments (Levine and Murrell 2003). The results presented here are consistent with previous theoretical studies of competition when there is no environmental heterogeneity; limiting dispersal slows growth rates and decreases the range of conditions allowing coexistence (Neuhauser and Pacala 1999; Bolker et al. 2003). It is difficult to judge their overall generality, because results here are derived for the lottery model in particular and make several assumptions that restrict interpretation, particularly concerning the symmetry of species (symmetrical dispersal and survival) and the mode of species-specific environmental response (through reproduction rates). It is also difficult to find empirical support for results, largely because of a lack of relevant studies. The spatial distribution of individuals (i.e., clustering) has been measured more often than underlying processes, such as environmental heterogeneity or species dispersal abilities (Archer et al. 1988; Rees et al. 1996; Idjadi and Karlson 2007; Sears and Chesson 2007; Raventós et al. 2010). These studies have shown that the covariance across space between growth rates and species densities favors coexistence, citing density-dependence in various demographic parameters as evidence (Rees et al. 1996; Sears and Chesson 2007; Raventós et al. 2010). Although theory suggests that limited dispersal can enhance the potential for coexistence in these cases, this depends on the extent that spatial variation in growth rates is driven by fixed environmental heterogeneity (Snyder and Chesson 2003). As favorable habitat becomes more ephemeral, species persistence is hindered by dispersal limitation. Changes in the spatial structure of density-dependence through time (e.g., a nonstationary spatial covariance) could indicate the overall stability of spatial heterogeneity, but determining the amount that dispersal limitation supplements or reduces coexistence in this context still requires additional studies.

Empirical support of the theoretical predictions made here could be found by extending existing studies. Evidence that dispersal limitation reduces coexistence by the temporal storage effect could be most directly obtained by experimentally manipulating dispersal in plant communities, such as desert annuals (Pake and Venable 1995; Angert et al. 2009). Here, direct comparisons of diversity and competitive effects could be made between a community where dispersal was naturally limited and one in which investigators collected seeds, mixed them, and distributed the mix evenly across plots. Direct experimental manipulation is less realistic for long-lived communities, such as tropical forests, where inferring long-term community dynamics may require a combination of long-term demographic data and models. The nucleation difference approximation is useful in this context, especially where previous studies of the storage effect could be supplemented with data on dispersal. Additionally, $\overline{B(p_1)}$ and $\overline{D(p_1)}$ could be determined from field data or fitted statistical models. This is amenable to an approach such as that used by Adler et al. (2010), where individual-based models and integral projection models were used to investigate coexistence in a perennial sagebrush community. Long-term, spatially explicit demographic data for this community were used to fit survival and growth curves of species as a function of their local neighborhoods. Because these survival and growth functions are neighborhood-dependent, they are analogous to the colonization and mortality probabilities in $\overline{B(p_1)}$ and $\overline{D(p_1)}$. The impact of dispersal limitation on coexistence could then be determined by using average dispersal distances to calculate new invasion growth rates from the nucleation difference equation and then comparing these to the invasion growth rates without dispersal limitation.

Dispersal limitation appears to drive trade-offs between coexistence mechanisms, increasing potential coexistence in spatial mechanisms (Bolker et al. 2003; Snyder and Chesson 2003) but decreasing it in nonspatial mechanisms (Neuhauser and Pacala 1999; Bolker et al. 2003; Levine and Murrell 2003). The relative importance of spatial and nonspatial mechanisms and the individual influences of simultaneous endogenous and exogenous processes on coexistence are largely unexplored. The theory presented here provides tools to assess the impact of dispersal limitation on the storage effect that are applicable to empirical analyses and complimentary to existing coexistence theory that quantifies the combined effect of endogenous and exogenous processes on vital rates (Rees et al. 1996; Chesson 2000a; Bolker et al. 2003; Snyder and Chesson 2003). Many communities where the storage effect is likely to operate are also those where dispersal limitation plays an important role in population dynamics; thus, it will be important to consider the full implications of dispersal limitation for coexistence on a community-by-community basis.

Acknowledgments

Literature Cited

Adler, P. B., S. P. Ellner, and J. M. Levine. 2010. Coexistence of perennial plants: an embarrassment of niches. Ecology Letters 13:1019–1029.

Adler, P. B., J. HilleRisLambers, P. C. Kyriakidis, Q. Guan, and J. M. Levine. 2006. Climate variability has a stabilizing effect on the coexistence of prairie grasses. Proceedings of the National Academy of Sciences of the USA 103:12793–12798.

Angert, A. L., T. E. Huxman, P. Chesson, and D. L. Venable. 2009. Functional tradeoffs determine species coexistence via the storage effect. Proceedings of the National Academy of Sciences of the USA 106:11641–11645.

Archer, S., C. Scifres, C. R. Bassham, and R. Maggio. 1988. Autogenic succession in a subtropical savanna: conversion of grassland to thorn woodland. Ecological Monographs 58:111–127.

Avrami, M. 1940. Kinetics of phase change. II. Transformation time relations for random distribution of nuclei. Journal of Chemical Physics 8:212.

Bolker, B. M. 2003. Combining endogenous and exogenous spatial variability in analytical population models. Theoretical Population Biology 64:255–270.

Bolker, B. M., S. W. Pacala, and C. Neuhauser. 2003. Spatial dynamics in model plant communities: what do we really know? American Naturalist 162:135–148.

Cáceres, C. E. 1997. Temporal variation, dormancy, and coexistence: a field test of the storage effect. Proceedings of the National Academy of Sciences of the USA 94:9171–9175.

Chesson, P. 2000*a*. General theory of competitive coexistence in spatially-varying environments. Theoretical Population Biology 58:211–237.

———. 2000*b*. Mechanisms of maintenance of species. Annual Review of Ecology and Systematics 31:343–366.

Chesson, P., R. L. Gebauer, S. Schwinning, N. Huntly, K. Wiegand, M. S. Ernest, A. Sher, et al. 2004. Resource pulses, species interactions, and diversity maintenance in arid and semi-arid environments. Oecologia 141:236–253.

Chesson, P. L., and R. R. Warner. 1981. Environmental variability promotes coexistence in lottery competitive systems. American Naturalist 117:923.

Clark, J. S., E. Macklin, and L. Wood. 1998. Stages and spatial scales of recruitment limitation in southern Appalachian forests. Ecological Monographs 68:213–235.

Cressie, N. A. C. 1993. Statistics for spatial data. Vol. 928. Rev. ed. Wiley Series in Probability and Mathematical Statistics. Wiley, New York.

Gandhi, A., S. Levin, and S. Orszag. 1999. Nucleation and relaxation from meta-stability in spatial ecological models. Journal of Theoretical Biology 200:121–146.

Godoy, O., and J. M. Levine. 2014. Phenology effects on invasion success: insights from coupling field experiments to coexistence theory. Ecology 95:726–736.

Gurney, W. S. C., and R. M. Nisbet. 1975. The regulation of inhomogeneous populations. Journal of Theoretical Biology 52:441–457.

Hiebeler, D. 1997. Stochastic spatial models: from simulations to mean field and local structure approximations. Journal of Theoretical Biology 187:307–319.

———. 2000. Populations on fragmented landscapes with spatially structured heterogeneities: landscape generation and local dispersal. Ecology 81:1629–1641.

Howe, H. F., and J. Smallwood. 1982. Ecology of seed dispersal. Annual Review of Ecology and Systematics 13:201–228.

Idjadi, J. A., and R. H. Karlson. 2007. Spatial arrangement of competitors influences coexistence of reef-building corals. Ecology 88:2449–2454.

Ishibashi, Y., and Y. Takagi. 1971. Note on ferroelectric domain switching. Journal of the Physical Society of Japan 31:506–509.

Ives, A. R., M. G. Turner, and S. M. Pearson. 1998. Local explanations of landscape patterns: can analytical approaches approximate simulation models of spatial processes? Ecosystems 1:35–51.

Kelly, C. K., and M. G. Bowler. 2002. Coexistence and relative abundance in forest trees. Nature 417:437–440.

Kemeny, J. G., and J. L. Snell. 1960. Finite Markov chains. Van Nostrand, London.

Korniss, G., and T. Caraco. 2005. Spatial dynamics of invasion: the geometry of introduced species. Journal of Theoretical Biology 233:137–150.

Korniss, G., C. J. White, P. A. Rikvold, and M. A. Novotny. 2000. Dynamic phase transition, universality, and finite-size scaling in the two-dimensional kinetic Ising model in an oscillating field. Physical Review E 63:016120.

Lavorel, S., and P. Chesson. 1995. How species with different regeneration niches coexist in patchy habitats with local disturbances. Oikos 74:103–114.

Levin, S. A., H. C. Muller-Landau, R. Nathan, and J. Chave. 2003. The ecology and evolution of seed dispersal: a theoretical perspective. Annual Review of Ecology, Evolution, and Systematics 34:575–604.

Levine, J. M., and D. J. Murrell. 2003. The community-level consequences of seed dispersal patterns. Annual Review of Ecology, Evolution, and Systematics 34:549–574.

MacArthur, R., and R. Levins. 1964. Competition, habitat selection, and character displacement in a patchy environment. Proceedings of the National Academy of Sciences of the USA 51:1207.

———. 1967. The limiting similarity, convergence, and divergence of coexisting species. American Naturalist 101:377–385.

Moran, P. A. P. 1950. Notes on continuous stochastic phenomena. Biometrika 37:17–23.

Muller-Landau, H. C., S. J. Wright, O. Calderón, R. Condit, and S. P. Hubbell. 2008. Interspecific variation in primary seed dispersal in a tropical forest. Journal of Ecology 96:653–667.

Neuhauser, C., and S. W. Pacala. 1999. An explicitly spatial version of the Lotka-Volterra model with interspecific competition. Annals of Applied Probability 9:1226–1259.

O'Brien, Sean T., Stephen P. Hubbell, Peter Spiro, Richard Condit, and Robin B. Foster. 1995. Diameter, height, crown, and age relationship in eight neotropical tree species. Ecology 76:1926–1939.

O'Malley, L., A. Allstadt, G. Korniss, and T. Caraco. 2005. Nucleation and global time scales in ecological invasion under preemptive competition. Proceedings of SPIE 5841:117–124.

Pake, C. E., and D. L. Venable. 1995. Is coexistence of Sonoran Desert annuals mediated by temporal variability reproductive success. Ecology 76:246–261.

Raventós, J., T. Wiegand, and M. D. Luis. 2010. Evidence for the spatial segregation hypothesis: a test with nine-year survivorship data in a Mediterranean shrubland. Ecology 91:2110–2120.

Rees, M., P. J. Grubb, and D. Kelly. 1996. Quantifying the impact of competition and spatial heterogeneity on the structure and dynamics of a four-species guild of winter annuals. American Naturalist 147:1–32.

Richards, H. L., S. W. Sides, M. Novotny, and P. A. Rikvold. 1995. Magnetization switching in nanoscale ferromagnetic grains: description by a kinetic Ising model. Journal of Magnetism and Magnetic Materials 150:37–50.

Rikvold, P. A., H. Tomita, S. Miyashita, and S. W. Sides. 1994. Metastable lifetimes in a kinetic Ising model: dependence on field and system size. Physical Review E 49:5080–5090.

Roberts, F. S. 1976. Discrete mathematical models: with applications to social, biological, and environmental problems. Prentice-Hall, Englewood Cliffs, NJ.

Sears, A. L., and P. Chesson. 2007. New methods for quantifying the spatial storage effect: an illustration with desert annuals. Ecology 88:2240–2247.

Seidler, T. G., and J. B. Plotkin. 2006. Seed dispersal and spatial pattern in tropical trees. PLoS Biology 4:e344.

Snyder, R. E., and P. Chesson. 2003. Local dispersal can facilitate coexistence in the presence of permanent spatial heterogeneity. Ecology Letters 6:301–309.

Snyder, R. E., and R. M. Nisbet. 2000. Spatial structure and fluctuations in the contact process and related models. Bulletin of Mathematical Biology 62:959–975.

Turelli, M. 1978. Does environmental variability limit niche overlap? Proceedings of the National Academy of Sciences of the USA 75: 5085–5089.

———. 1981. Niche overlap and invasion of competitors in random environments. I. Models without demographic stochasticity. Theoretical Population Biology 20:1–56.

Usinowicz, J., S. J. Wright, and A. R. Ives. 2012. Coexistence in tropical forests through asynchronous variation in annual seed production. Ecology 93:2073–2084.

Vance, R. R. 1978. Predation and resource partitioning in one predator–two prey model communities. American Naturalist 112:797–813.

Venable, D. L., A. Flores-Martinez, H. C. Muller-Landau, G. Barron-Gafford, and J. X. Becerra. 2008. Seed dispersal of desert annuals. Ecology 89:2218–2227.

White, G. M. 1969. Steady state random walks with application to homogeneous nucleation. Journal of Chemical Physics 50:4672.

Associate Editor: Benjamin M. Bolker
Editor: Troy Day
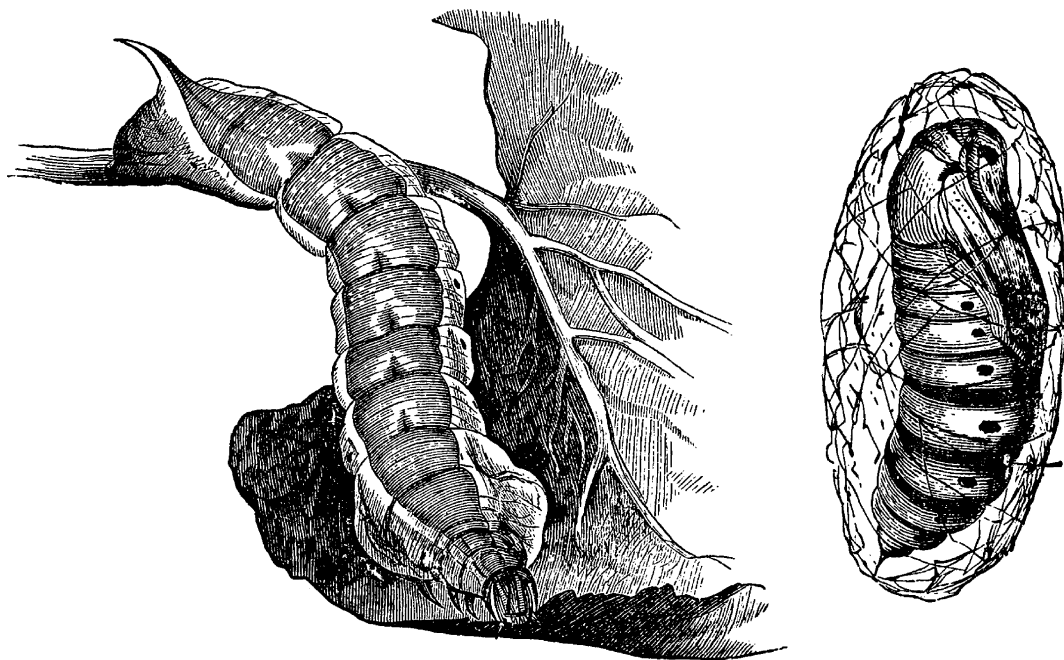
"A true knowledge of practical entomology may well be said to be in its infancy, when, as is well known to agriculturists, the cultivation of wheat has almost been given up in portions of the northern states from the attacks of the wheat midge, Hessian fly, joint worm and chinch bug. . . . A single caterpillar of [the Vine dresser (*Chœrocampa pampinatrix* Smith and Abbott), illustrated] will sometimes 'strip a small vine of its leaves in a few nights,' and sometimes nips off bunches of half-grown grapes." From "Review: Economical Entomology in Missouri" (*The American Naturalist*, 1870, 4:610–615).